Power Sharing in an Islanded Single-Phase Microgrid: Performance Analysis of Droop Control Strategies

Gerard Beral, Allal El Moubarek Bouzid, Corinne Alonso, David Tsuanyo, Pierre Tsafack

Power Sharing in an Islanded Single-Phase Microgrid: Performance Analysis of Droop Control Strategies

Gerard BERAL · Allal El Moubarek BOUZID · Corinne ALONSO · David TSUANYO · Pierre TSAFACK

Abstract For the smooth operation of microgrids (MGs), an efficient power sharing strategy is crucial to maintain the frequency and voltage regulation of distributed generators (DGs) within specified deviation limits. The droop control strategy is widely adopted to share power in microgrid applications. This paper presents a comparative study between conventional droop control (CDC) and universal droop control (UDC). The main objective of this study is to evaluate the performance of these droop control methods in scenarios involving DGs Plug & Play and load variations. Issues of frequency and voltage deviations are explored to ensure compliance with international microgrid standards. Simulations were conducted using a virtual Hardware-in-the-Loop (VHIL) on Typhoon HIL. An islanded single-phase microgrid integrating renewable energy through four distributed generators was used. The results demonstrate that both controllers are suitable candidates for effectively allocating real and reactive powers with varying levels of accuracy.

1 Introduction

In recent years, single-phase microgrids have become recognized as a practical and sustainable solution for delivering a power supply to diverse applications, ranging from buildings to small communities in both urban and rural area [1]. These MGs present a solution for effectively harnessing and hybridizing the numerous energy resources available within these communities. However, the simultaneous utilization of distributed energy resources (DERs) can introduce several challenges, such as power sharing and concerns related to frequency and voltage stability. In the literature, droop control is widely used to share active and reactive power among distributed generator units in parallel. This technique is easy to be implemented and achieves high reliability and flexibility [2]. Its principle mimics a synchronous generator and can only be applied to inverters with inductive output impedance.

However, real power plant systems have different types of inverters based on the output impedance (R, L, C, and mixed). In distribution networks, such as standalone MGs, the impedance could be predominantly resistive. In this scenario, the CDC exhibits poor performance [1]. Also it presents a poor power quality for non-linear or asymmetrical loads [3]. To improve the CDC, researchers have proposed several techniques to overcome voltage and frequency deviations and dependence on the output impedance of inverters. The virtual impedance method was developed to force the output impedance to be inductive [4]. The robust or universal droop controller (UDC) was introduced. It can cover a wide range of inverters with different types of output impedance [5,6]. A nonlinear or quadratic droop, proposed in [7], was designed to handle non-linear behaviors of the MG. However for proper implementation, it requires accurate model of MG. The nonlinear droop and others improved droop are studied in [3,8]. They may rely on high computational requirements and additional communication loops . However in real systems, efficiency, communication-free operation, reliability, robustness, and good applicability are generally preferred.

In this study, the CDC and UDC implemented in an islanded single-phase microgrid are investigated in steady and transient states, with a particular focus on the steady state. The performance of the controllers is tested through various scenarios, including DGs plug & play and load variations. Firstly, after introducing the primary control of microgrids, a comparison between CDC and UDC is presented. Moreover, emphasis was placed on the importance of droop controllers satisfying the re-

G. Beral · C. Alonso
LAAS-CNRS
7 Av. du Colonel Roche, 31400 Toulouse, France
Université Toulouse III , CNRS, UPS, Toulouse, France
118 Rte de Narbonne, 31062 Toulouse
Institut Ucac-Icam
BP 5504 Douala, Cameroun
e-mail: gerard.beral@ucac-icam.com, corinne.alonso@laas.fr,

A. Bouzid · P. Tsafack
LAAS-CNRS
Icam site de Toulouse
e-mail: allal.bouzid@icam.fr

quirements of international standards and norms, such as IEEE 1547 [9] and IEC 60034-1. These standards specify the highest allowed deviation of frequency and voltage from the nominal values (i.e., $\pm 2\%$ and $\pm 5\%$, respectively). Subsequently, small signal models of the controllers are determined, followed by the discussion of simulation results. Finally, conclusions and future directions are outlined.

2 Microgrid and primary control

Several definitions have been presented for a MG, according to CIGRE, it can be defined as sections of electricity distribution systems containing loads and distributed energy resources (such as DGs, storage devices, or controllable loads) that can be operated in a controlled, coordinated way, either while connected to the main grid and/or while islanded [10]. MGs technologies are facilitating the effective integration of both dispatchable and non-dispatchable energy sources, including small hydro, solar, wind, and bio sources, with the aim of significantly reducing the reliance on fossil fuels. The development of MGs involves efficient control strategies for their components, such as DGs or converters.

Depending on the control strategies, the converter can operate as current source (maintaining stable current while voltage changes). It is referred to as grid feeding/following. The grid feeding finds application in grid connected systems [11]. It cannot be able to work alone in standalone system. The grid forming has been introduced to tackle this issue, acting as voltage source (maintaining stable voltage while current changes). So the grid forming is very important for islanded MGs. The grid supporting/conditioning includes both grid forming and feeding functions. It can provide ancillary services [12].

Numerous control strategies for grid forming have been developed to ensure the frequency and voltage stability of DGs. These include the virtual synchronous generator (VSG), the dispatchable virtual oscillator (DVOC), the machine matching control (MMC), and the droop control [11, 12]. VSG simulates the complete dynamic behavior of synchronous generators including inertia. The DVOC is realized with Van der Pol oscillator dynamics, which is a specific example of a Liénard-type oscillator. The machine matching control is an emerging control technique that aims to establish, a coupling between the frequency and active power balance by achieving a crucial coupling between the DC-side voltage and the AC-side frequency [12]. The droop control, VSG, and DVOC are considered as the main types of primary controllers [13]. While the droop control is the most commonly used method for power sharing in standalone systems.

3 Conventional droop controller

Centralized, hierarchical, and distributed control strategies depend on communication links to enhance the quality of sensor measurements. Their main drawback is the single point of failure (SPF), which can introduce an instability in the grid when communication systems encounter issues such as data delays or loss [14]. Therefore, communication-free or decentralized control strategies such as droop find extensive application. This is particularly suitable for power sharing among DGs in microgrids in remote areas. A DG unit can be represented by an equivalent circuit diagram, as shown in Fig. 1. According to [5], its active and reactive power expressions are

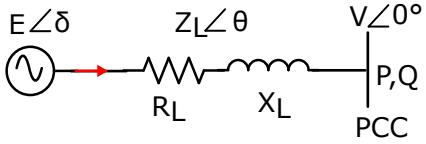

Fig. 1: Equivalent circuit diagram of a DG unit

$$\begin{cases} P = \left(\frac{EV}{Z_L}\cos(\delta) - \frac{V^2}{Z_L}\right)\cos(\theta) + \frac{EV}{Z_L}\sin(\theta)\sin(\delta) \\ Q = \left(\frac{EV}{Z_L}\cos(\delta) - \frac{V^2}{Z_L}\right)\sin(\theta) - \frac{EV}{Z_L}\cos(\theta)\sin(\delta) \end{cases} \tag{1}$$

where δ is the phase difference between the supply side and AC bus, $Z_L = R_L + jX_L$ is the output impedance, V and E are the voltage amplitudes of the AC bus and the DG source, respectively. According to (1), the nature of the output impedance can vary, leading to a mismatched impedance between DGs. This restricts the application of conventional droop, which is effective for systems with inductive outputs such as high-voltage or grid-connected MGs. In low-voltage distribution networks or islanded microgrids, the average value of the R/X ratio highlights the predominantly resistive nature of the impedance. Consequently, either a real or virtual inductive impedance becomes necessary. Considering selection criteria such as cost and space constraints, the virtual solution emerges as the most preferred option. By incorporating a virtual impedance into the control loop to ensure that Z_L becomes purely inductive ($\theta = 90^\circ$) and neglecting R_L, (1) becomes

$$\begin{cases} P = \frac{EV}{X_L}\sin(\delta) \\ Q = \frac{EV}{X_L}\cos(\delta) - \frac{V^2}{X_L} \end{cases} \tag{2}$$

To apply the $(P-\omega/Q-V)$ droop in (2), the active and reactive power need to be measured and filtered. The second-order generalized integrator-based frequency-locked loop (SOGI-FLL) was utilized for power calculation. This method extracts the orthogonal components $v_{\alpha\beta}$ and $i_{\alpha\beta}$ from the output voltage and current of each DG unit [15]. The expressions for average active and reactive powers are

$$\begin{cases} P = 0.5\left(\hat{v}_\alpha \times \hat{i}_\alpha + \hat{v}_\beta \times \hat{i}_\beta\right) \\ Q = 0.5\left(\hat{v}_\beta \times \hat{i}_\alpha - \hat{v}_\alpha \times \hat{i}_\beta\right) \end{cases} \tag{3}$$

Subsequently, the active and reactive powers are measured using a low-pass filter (LPF). To effectively suppress high-frequency

components, the cutoff frequency of filter must be considerably lower than the frequency of inner loop. The extracted and filtered power is then directly utilized in the droop control block:

$$\begin{cases} \omega = \omega_{\text{ref}} - m(P_{\text{meas}} - P_{\text{ref}}) \\ E = E_{\text{ref}} - n(Q_{\text{meas}} - Q_{\text{ref}}) \end{cases} \tag{4}$$

Where

$$\begin{cases} 0 < m \leq \frac{\omega_{\max} - \omega_{\min}}{P_{\text{rated}}} \\ 0 < n \leq \frac{V_{\max} - V_{\min}}{Q_{\text{rated}}} \end{cases} \tag{5}$$

ω_{ref} and E_{ref} are the nominal values of angular frequency and voltage, m and n are the active and reactive droop slopes, respectively. P_{meas} and Q_{meas} are the measured averaged real and reactive power. As a global parameter and nearly constant in the power system, the frequency enables accurate active power sharing. The voltage, on the other hand, is a local parameter influenced by mismatched feeder impedance between the DGs and loads. Consequently, the voltage varies from one point to another. As a result, the reactive loop exhibits poor performance in voltage and reactive power regulation, potentially leading to circulating current among DGs.

4 Universal droop controller

A robust droop control is specifically designed to be robust against numerical errors, disturbances, noises, feeder impedance, and component mismatches [16]. Originally developed for resistive inverters, robust droop control has since been found to be effective with any type of output impedance [5]. It can be applied to inverters with an impedance angle between $-\frac{\pi}{2}$ and $\frac{\pi}{2}$ without the need to know or measure the output impedance values. Therefore, it has become universal, representing a better solution for addressing parameter disparities in power systems. There are various methods to implement the universal droop

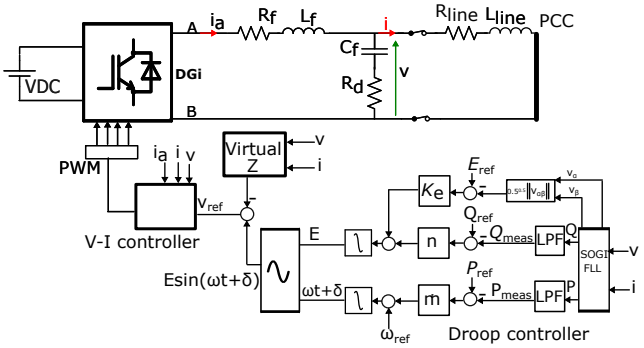

Fig. 2: Implemented UDC

control principle. In this paper, the implemented UDC, as depicted in Fig. 2, is combined with a virtual inductive impedance.

The equation describing the UDC law is given by:

$$\begin{cases} \dot{E} = (E_{\text{ref}} - V)k_e - n(Q_{\text{meas}} - Q_{\text{ref}}) \\ \dot{(\omega t + \phi)} = \omega_{\text{ref}} - m(P_{\text{meas}} - P_{\text{ref}}) \end{cases} \tag{6}$$

The power references are set such that $Q_{\text{ref}} = 0$ and $P_{\text{ref}} = 0$

$$V = \frac{\|v_{\alpha\beta}\|}{\sqrt{2}} = \frac{\sqrt{v_\alpha^2 + v_\beta^2}}{\sqrt{2}} \tag{7}$$

While k_e is a constant acting as proportional controller by reducing error in measurement of V.

In the steady state ($\dot{E} = 0$), V is analysed in terms of k_e:

$$V = E_{\text{ref}} - \frac{n \cdot Q_{\text{meas}}}{k_e} \tag{8}$$

It can be observed in the steady state, the voltage (V) is determined by the reference voltage (E_{ref}), the measured reactive power (Q_{meas}), and the constants k_e and n. To achieve $E_{\text{ref}} \approx V$, the values of n and k_e must be selected such that their ratio $\frac{n}{k_e}$ is minimized, meaning choosing a large k_e. This ensures that the term $\frac{n \cdot Q_{\text{meas}}}{k_e}$ has a minimal impact on V. Optimal values for n and k_e will depend on specific system requirements. Generally, aiming for a small droop gain ($\frac{n}{k_e}$) and restricting variations in Q_{meas} contribute to the desired behavior where E_{ref} is nearly equal to V. According to (8), the UDC could better achieve voltage regulation within predetermined ranges compared to CDC. Therefore, a method to properly tune the ratio $\frac{n}{k_e}$ is required to force the two-integrator to achieve better performance against voltage fluctuations which could damage power systems, such as rapid voltage change (RVC), which commonly occurs in LV and MV distribution networks [17].

The stability of power systems passing through controllers capable of meeting voltage and frequency regulation within predetermined ranges, as stipulated by international standards, is crucial. Grid solutions like microgrids, Virtual Power Plants (VPPs), updated and extended conventional grids are experiencing rapid growth. The interconnected world of smart grids, sharing clean and sustainable energy as outlined by SDG7 (Sustainable Development Goal 7) is imminent. In anticipation of the future interconnection and interoperability of global grid networks, a common framework for DER and microgrid standards is necessary [9]. Therefore, it is important for droop control and other techniques to meet international standard requirements (IEEE 1547, IEC 60034-1, etc.). This standardization is essential to guarantee the safe operational conditions of DER when integrated with other power systems.

5 Small signal analysis

The small signal performance was investigated around singular or equilibrium points (ω_e, V_e, E_e, P_e, Q_e). The goal is to develop small signal models for the UDC across various ranges of k_e values. Two cases were considered to study (8). In case 1, considering large values of k_e implies a constant V, whereas in case 2, small values of k_e suggest potential variations in V. To simplify small signal modeling, only the first-order derivative terms of Taylor series will be utilized. The dynamic behavior

of inverters was neglected, and only droop controller models will be examined.

Firstly, considering case 1, the law (4) of CDC can be linearized around the equilibrium point :

$$\begin{cases} s\Delta\omega(s) = -\omega_f \Delta\omega(s) - m\omega_f \Delta P(s) \\ s\Delta E(s) = -\omega_f \Delta E(s) - n\omega_f \Delta Q(s) \end{cases} \quad (9)$$

Where $(\omega_f / \omega_f + s)$ represents the low-pass filter (LPF) used to measure P and Q. The linearized equation of (6) of the UDC is identical to (9), indicating that CDC and UDC share the same small signal model. In case 2, the CDC maintains the same model as in case 1. Meanwhile, the model of UDC has evolved, considering load variations. Similarly, as presented in [18], the linearized form of (6) is

$$\begin{cases} s\Delta\omega(s) = -\omega_f \Delta\omega(s) - m\omega_f \Delta P(s) \\ s\Delta E(s) = -\omega_f \Delta E(s) - \omega_f K_e \Delta V(s) - K_e s\Delta V(s) \\ -n\omega_f \Delta Q(s) \end{cases} \quad (10)$$

Now, V is a variable, therefore two extra terms related to the deviation ΔV and its derivative are included in the UDC small signal model. This UDC small signal model will facilitate the study and comprehension of MG behavior under small load variations.

6 Simulations and results

The studied system in Fig. 3, is a single-phase microgrid with 4 DGs, including RL and R loads. Each DG comprises a DC source, single-phase inverters, an LC filter, and a feeder line output impedance. The comparison of CDC and UDC, combined with virtual impedance was carried out through VHIL simulation. This aims to observe the transient and steady-state of both controllers. The connection and disconnection of DGs are performed. Frequency and voltage deviation issues are analyzed with the goal of ensuring if the controllers meets the IEEE 1547 requirements. The R and RL loads were chosen as they are the most common load types in power systems.

The droop slopes (m and n) were defined based on the highest allowed deviation of V/f from the nominal values (5% and 2%,respectively). The simulations were conducted in multiple steps with Matlab and Typhoon HIL. Firstly, a Virtual Hardware in the Loop (VHIL) model of the microgrid was built. Next, it was transferred to the Hardware in the Loop (HIL) SCADA. The resulting data were exported as a CSV file, which was then processed by a Matlab script. Finally, a graph was generated. The MG operations are simulated through following scenarios:

6.1 Scenario 1: Load variations

In this scenario, a test was conducted involving a change in load values and type by introducing an R load (41 kW) and an RL load (4.9 kW, 18.5 kVAR). Initially, with no load, all DGs were connected. At t = 0.5 s, the R load was connected, and it was disconnected at t = 0.9 s. Then, at t = 1 s, the RL load was connected, and it was finally disconnected at t = 1.5 s. The IEEE 1547 standard specifies the maximum allowable deviation of frequency and voltage from their nominal values, which are $\pm 2\%$ and $\pm 5\%$, respectively. For the studied system with nominal values of 220 V/60 Hz, it is necessary for both the frequency and voltage to remain within a range of 58.8 Hz to 61.2 Hz and 209 V to 231 V respectively.

In the steady state, as depicted in Fig. 4 and Fig. 5, the output powers of each DGs are equal, indicating that both active and reactive powers are properly shared by both controllers. The frequency and voltage values of DGs controlled by UDC are 215 V/59.6 Hz under the R load and 215 V/60 Hz with the RL load, which are within the acceptable range defined by IEEE 1547. Conversely, DGs controlled by CDC have voltage and frequency values of 212 V/59.6 Hz (satisfying the standard) with the R load and 200 V/60 Hz (the voltage does not meet the standard) under the RL load. So the UDC is better than CDC in Voltage regulation, this is also illustrated in Fig. 8 and Fig. 9. These results confirm the impact of the new parameter k_e. By properly selecting the values of droop gains and k_e, errors in the steady state could effectively be mitigated. Therefore, the key is to establish a procedure for selecting appropriate values of k_e.

In the transient state, as illustrated in Fig. 8 and Fig. 9, with the CDC, a dangerous over-voltage can occur when disconnecting or connecting loads, while the UDC does not exhibit such behavior. In the end, both controllers demonstrate similar performance in frequency regulation, with the frequency values satisfying the IEEE 1547 standard.

6.2 Scenario 2: Plug and play test

The two controllers are tested regarding their capability to handle the connection and disconnection of DGs. Initially, DG1 and DG2 were connected to the AC bus, and then a resistive load was added at t = 0.4 s. Subsequently, DG3 was connected at t = 0.9 s, followed by the addition of an RL load at t = 1.4 s. Finally, DG4 was connected at t = 2 s, and DG3 was removed at t = 2.5 s.

Table 1: DG unit Parameters

Parameter	**Value**
Nominal DC bus voltage	400 V
Nominal voltage	220 V
Nominal frequency	60 Hz
Rated apparent power	33KVA
Switching frequency	10 kHz
Frequency deviation	$\pm 2\%$
Voltage deviation	$\pm 5\%$
Droop gain (m)	$2.4\pi \frac{1}{33\times10^3}$
Droop gain (n)	$\frac{11}{33\times10^3}$
L filter	0.25 mH
C filter	100 μF
L line feeder	20 μH
R line feeder	10 mΩ

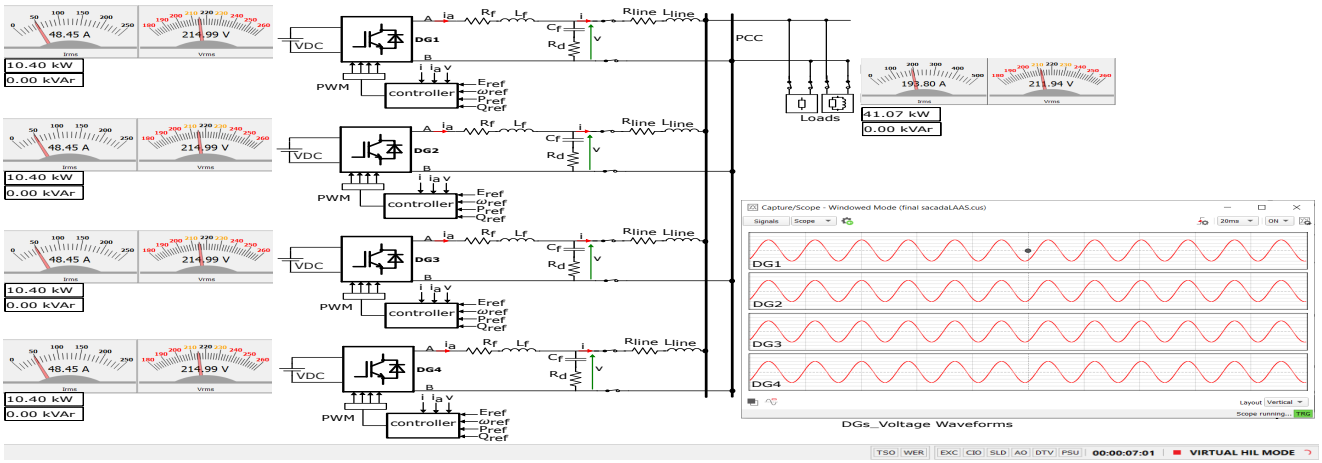

Fig. 3: Studied system:Measurement of MG parameters

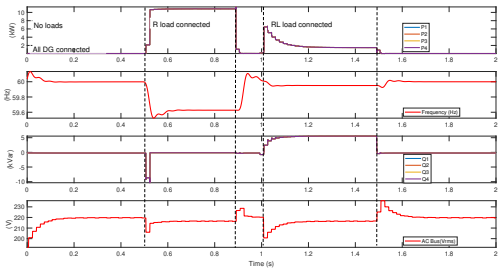

Fig. 4: UDC: Power sharing during load variations

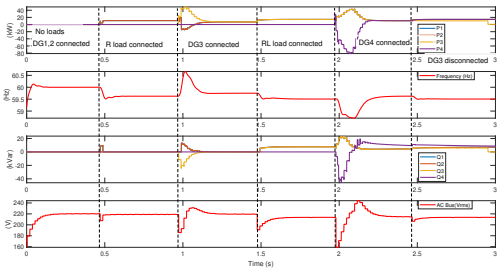

Fig. 6: UDC: Behavior of DGs during plug-and-play test

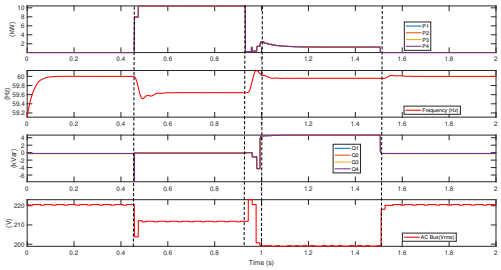

Fig. 5: CDC: Power sharing during load variations

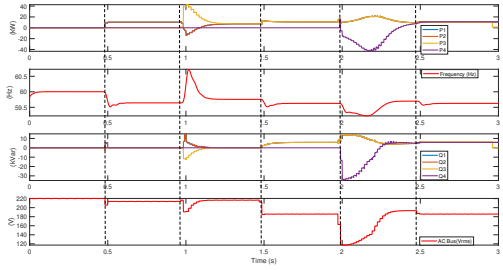

Fig. 7: CDC: Behavior of DGs during plug-and-play test

In the steady state, as depicted in Fig. 6 and Fig. 7, both controllers demonstrate the same behavior as discussed in scenario 1. Additionally, they exhibit plug-and-play features.

In the transient state, the voltage of DGs controlled by the UDC drops from 220 V to 180 V at t = 1 s and 160 V at t = 2 s as shown in Fig. 6 and Fig. 7. At the same time, the voltage from CDC drops to 198 V and 120 V, respectively. The CDC exhibits the most significant voltage drop. However, both controllers fail to satisfy the IEEE 1547 standard, especially during DGs connection.When connecting a DG, the rate of change of frequency (RoCoF) and rate of change of voltage (RoCoV) are more pronounced in conventional droop control compared to universal droop. According to these results, when multiple DGs with the same rating are operating in parallel, a DG disconnection operation is seamless in both controllers. However, the connection operation can lead to a significant RoCoF and RoCoV. Universal droop control handles disconnections and connections more effectively compared to conventional droop.

7 Conclusion

In this study, the performance of conventional droop and a variant of universal droop control was examined in a single-phase

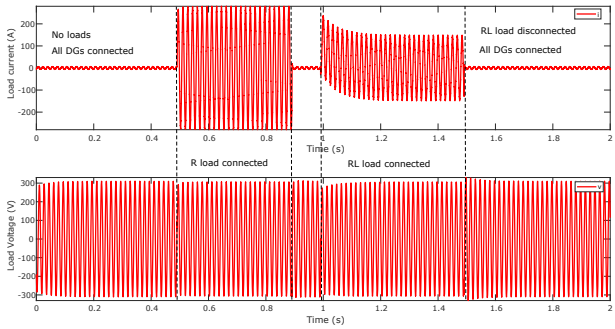

Fig. 8: UDC: Voltage and current waveforms during load variations

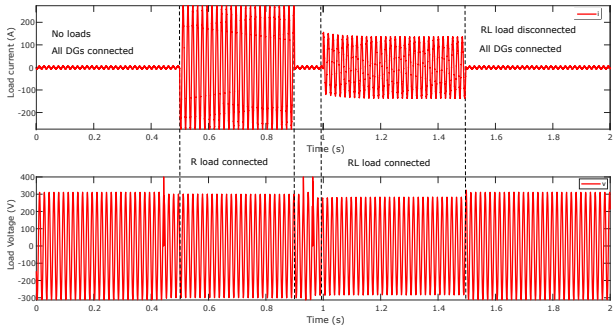

Fig. 9: CDC: Voltage and current waveforms during load variations

islanded microgrid. Evaluations address both steady-state and transient conditions, considering load variations and the connection and disconnection of distributed generators, with the goal of meeting IEEE standard 1547. Universal droop demonstrates efficient voltage regulation in steady-state, and it exhibits superior transient behavior during DGs connection and disconnection. Consequently, the RoCoF and RoCoV are more pronounced in conventional droop than in universal droop. The small signal models of the UDC were determined, considering both constant load voltage and variations in load voltage. Future directions for this work include the development of a method or procedure for selecting appropriate values of k_e and conducting eigenvalues analysis of the determined small signal models. Additionally, testing CDC and UDC under abnormal conditions such as overloading and the unplanned connection and disconnection of distributed generators using Hardware-in-the-Loop simulations should be explored.

References

1. ALHAIZ, Hussain A., ALSAFRAN, Ahmed S., et ALMARHOON, Ali H.Single-Phase Microgrid Power Quality Enhancement Strategies: A Comprehensive Review.*Energies, 2023*, vol. 16, no 14, p. 5576.
2. GUERRERO, Josep M., VASQUEZ, Juan C., MATAS, José, et al.Hierarchical control of droop-controlled AC and DC microgrids—A general approach toward standardization.*IEEE Transactions on industrial electronics, 2010* , vol. 58, no 1, p. 158-172.
3. SRIVASTAVA, Sumit, RAVI, Guguloth, TRIPATHI, Pushkar, et al.Droop Control based Control technique and Advancements for Microgrid Stability-A Review.In : *2023 IEEE Renewable Energy and Sustainable E-Mobility Conference (RESEM)* . IEEE, 2023. p. 1-6.
4. HAN, Yang, SHEN, Pan, ZHAO, Xin, et al.Control strategies for islanded microgrid using enhanced hierarchical control structure with multiple current-loop damping schemes.*IEEE Transactions on Smart Grid, 2015* , vol. 8, no 3, p. 1139-1153.
5. ZHONG, Qing-Chang et ZENG, Yu.Universal droop control of inverters with different types of output impedance.*IEEE access, 2016* , vol. 4, p. 702-712.
6. TAYAB, Usman Bashir, ROSLAN, Mohd Azrik Bin, HWAI, Leong Jenn, et al. A review of droop control techniques for microgrid.*Renewable and Sustainable Energy Reviews, 2017* , vol. 76, p. 717-727.
7. Simpson-Porco, John W., et al. Voltage Stabilization in Microgrids via Quadratic Droop Control.*IEEE Transactions on Automatic Control, 2017* , vol. 62, no. 3, pp. 1239–53.
8. ISHAQ, Saima, KHAN, Irfan, RAHMAN, Syed, et al.A review on recent developments in control and optimization of micro grids.*Energy Reports, 2022* , vol. 8, p. 4085-4103.
9. REBOLLAL, David, CARPINTERO-RENTERÍA, Miguel, SANTOS-MARTÍN, David, et al.Microgrid and distributed energy resources standards and guidelines review: Grid connection and operation technical requirements.*Energies, 2021* , vol. 14, no 3, p. 523.
10. ABBASI, Maysam, ABBASI, Ehsan, LI, Li, et al.Review on the microgrid concept, structures, components, communication systems, and control methods.*Energies, 2023* , vol. 16, no 1, p. 484.
11. Harasis, Salman.Controllable Transient Power Sharing of Inverter-Based Droop Controlled Microgrid.*International Journal of Electrical Power $_E$nergySystems*,2024,*vol*.155,*p*.109565.*BOUZID*,*AllalM*.,*GUERRERO*,*J*
766.
12. ANTTILA, Sara, DÖHLER, Jéssica S., OLIVEIRA, Janaína G., et al.Grid forming inverters: A review of the state of the art of key elements for microgrid operation.*Energies, 2022* , vol. 15, no 15, p. 5517.
13. PEREIRA, Alexandre T., PINHEIRO, Humberto, STEFANELLO, Márcio, et al.Microgrid Primary Controller Performance Characterization. Real-Time Simulation and Hardware-in-the-Loop Testing Using Typhoon HIL 2023, p. 211-254.
14. ZUO, Kunyu et WU, Lei. A review of decentralized and distributed control approaches for islanded microgrids: Novel designs, current trends, and emerging challenges. *The Electricity Journal, 2022* , vol. 35, no 5, p. 107138.
15. BENDIB, Ahmed, CHOUDER, Aissa, KARA, Kamel, et al.New modeling approach of secondary control layer for autonomous single-phase microgrids.*Journal of the Franklin Institute, 2019* , vol. 356, no 13, p. 6842-6874.
16. Zhong, Qing-Chang.Robust Droop Controller for Accurate Proportional Load Sharing Among Inverters Operated in Parallel.*IEEE Transactions on Industrial Electronics,2013* ,vol. 60, no. 4, pp. 1281–90.
17. SEPASI, Saeed, TALICHET, Celia, et PRAMANIK, Abrar S.Power Quality in Microgrids: A Critical Review of Fundamentals, Standards, and Case Studies.*IEEE Access, 2023*
18. Coelho, E. A., Wu, D., Guerrero, J. M., Vasquez, J. C., Dragicevic, T., Stefanović, C., Popovski, P. (2016). Small-signal analysis of the microgrid secondary control considering a communication time delay.*IEEE Transactions on Industrial Electronics*, 63(10), 6257-6269.